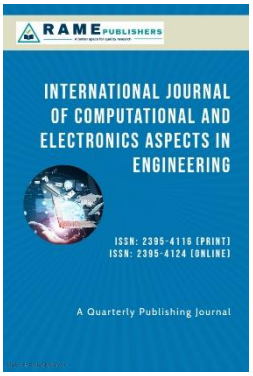
International Journal of Computational and Electronics Aspects in Engineering
Volume 7, Issue 5, November 2026, pp 588 - 603
https://doi.org/10.26706/ijceae.7.5.20261005

IoT-Based Intelligent Energy Management for Hybrid PV–Battery–Grid Homes under Intermittent Grid Supply

Abdulla Mohannad Habbib

Department of Medical Instrumentation Techniques Engineering, Polytechnic College Mosul, Northern Technical University, Mosul, Iraq. https://orcid.org/0009-0000-3273-5560

***Correspondence:** abdulla1985@ntu.edu.iq



Abstract: Households in Iraq face rotating grid outages and depend on capacity-limited neighbourhood diesel generators, while rooftop photovoltaic (PV)–battery systems are usually operated by fixed inverter rules that ignore the outage schedule. This paper designs an Internet-of-Things (IoT) energy management system for a PV–battery–grid–generator home. It comprises four ESP32 nodes, an MQTT network and an edge gateway that runs an outage-aware model-predictive controller (MPC), formulated as a linear programme and executed through the time-of-use registers of Deye/Sunsynk hybrid inverters. The system was evaluated by a full-year hourly simulation for a Baghdad house driven by 2023 irradiance and temperature data, comparing six strategies over three random realisations of demand and outages. A conventional self-use rule left 6.4% of the demand unserved, whereas an outage-aware rule and the proposed IoT-MPC served practically all demand. Relative to the rule, the IoT-MPC reduced grid imports by 23.6%, PV curtailment by 19.7% and battery cycling by 17.9%, and raised self-sufficiency from 45.2% to 52.7%; each optimisation took 4.8 ms. A 10 kWh battery allowed the generator subscription to be halved, lowering the annual energy cost by about 40%. Outage-aware predictive control therefore delivers equal reliability with markedly lower grid use and battery wear.

Keywords: home energy management; Internet of Things; model predictive control; photovoltaic; battery storage; intermittent grid; ESP32; MQTT; Iraq

Article – Peer Reviewed
Received: 5 August 2026
Accepted: 9 October 2026
Published: 3 November 2026

Copyright: © 2026 RAME Publishers
This is an open access article under the CC BY 4.0 International License.

https://creativecommons.org/licenses/by/4.0/

Cite this article: Abdulla Mohannad Habbib, "IoT-Based Intelligent Energy Management for Hybrid PV–Battery–Grid Homes under Intermittent Grid Supply", *International Journal of Computational and Electronic Aspects in Engineering*, RAME Publishers, vol. 7, issue 5, pp. 588-603, 2026.
https://doi.org/10.26706/ijceae.7.5.20261005

1. Introduction

Reliable electricity remains one of the most pressing problems facing Iraqi households. Although installed generation capacity has grown, the national grid cannot meet peak demand, and in summer, when air-conditioning drives consumption to its highest level, distribution companies apply rotating supply schedules of the type "two hours on, two hours off" [1], [2]. Households bridge the gaps with neighbourhood diesel generators. These are operated privately and sold as monthly subscriptions per ampere, for example 9,000 IQD per ampere per month for an 18-hour line in Baghdad in June 2023 [3]. The resulting supply is expensive, noisy and polluting, and it is capped by the subscribed current. At the same time, the residential grid tariff is heavily subsidised (10 IQD/kWh for the residential rate [4]), so grid energy is extremely cheap whenever it is available.

Iraq has an excellent solar resource, with global horizontal irradiation of about 1,900 kWh/m² per year in Baghdad, and rooftop PV with lithium-iron-phosphate ($LiFePO_4$) batteries has become an attractive way to ride through outages [5], [6]. The hybrid inverters on the market, however, are typically operated in a fixed mode, such as "self-use" (discharge whenever PV is insufficient) or "backup" (keep the battery full). Neither mode knows when the next outage will occur or how much energy it will require. A self-use battery is often empty when the grid fails, and a backup battery is permanently full, wastes surplus PV and charges from the grid unnecessarily.

A home energy management system (HEMS) can resolve this conflict by combining measurements, forecasts and optimisation [7]–[9]. Model-predictive control (MPC), which

repeatedly solves a finite-horizon optimisation and applies only the first decision, has been used successfully for microgrids and residential batteries [10], [11]. The Internet of Things (IoT) provides the low-cost sensing, communication and actuation needed to implement such controllers in ordinary homes [12]. Most published HEMS studies, however, assume a reliable grid with time-of-use prices and treat outages as rare contingencies. Few address the "weak-grid" condition of Iraq and similar countries, where outages are scheduled, frequent and partly announced, and where a capacity-limited generator is a third source.

This paper addresses that gap. Its contributions are as follows:

1. A complete IoT architecture is designed for a PV–battery–grid–generator household. It comprises four ESP32 nodes for metering, inverter communication, load switching and grid sensing, an MQTT network, and an edge gateway, together with a bill of materials, a message schema and reference firmware.
2. An outage-aware rolling-horizon MPC is formulated as a linear programme. It exploits the announced grid schedule, includes a soft energy reserve against unannounced outages, accounts for the generator's ampere limit and operating window, and schedules shiftable appliances.
3. A practical execution layer maps the MPC decisions onto the six-slot time-of-use program of widely used Deye/Sunsynk hybrid inverters, with the Modbus register map, a dynamic-programming compression of the daily plan into six slots, and a reference firmware. This lets the controller run on existing inverters without modifying their firmware.
4. The system is evaluated by a full-year, hourly simulation for a Baghdad household, driven by hourly irradiance and temperature for 2023 from the ERA5-based Open-Meteo archive. Six control strategies, including two common inverter rules and an MPC with perfect forecasts, are compared over three random realisations of demand and outages.
5. Sensitivity analyses of battery capacity, generator subscription and grid tariff quantify the economic value of the system under current and reformed Iraqi tariffs.

The remainder of the paper is organised as follows. Section 2 reviews related work. Section 3 presents the system and IoT design. Section 4 describes the models and data, and Section 5 the control strategies. Section 6 reports the results, Section 7 discusses them, and Section 8 concludes.

2. Related Work

Home energy management systems. Zhou et al. [7] reviewed HEMS concepts, configurations and scheduling strategies, and Shareef et al. [8] surveyed HEMS with demand response, smart technologies and intelligent controllers. Pipattanasomporn et al. [9] proposed an early algorithm that keeps household demand below a limit by prioritising appliances, which is conceptually close to managing a capacity-limited generator. Luthander et al. [13] showed that batteries and load management can raise PV self-consumption substantially, which is the main objective of most HEMS in reliable grids. Artificial-intelligence methods for PV forecasting, maximum-power-point tracking and energy management have been reviewed recently [14], [15], and energy storage combined with active filtering has been shown to improve the power quality of grid-connected hybrid solar–wind systems [16].

Model-predictive control. Parisio et al. [10] formulated microgrid operation as a mixed-integer MPC and demonstrated its advantage over heuristic dispatch. Mariano-Hernández et al. [11] reviewed MPC, demand-side management and optimisation in building energy management and identified forecast uncertainty and computational effort as the main barriers to adoption. Linear formulations solved by modern solvers such as HiGHS [17] make MPC feasible on embedded hardware.

IoT-based energy management. Al-Ali et al. [12] implemented a smart-home EMS with IoT devices and data analytics and showed that low-cost microcontrollers and cloud services are sufficient for monitoring and control. The MQTT publish/subscribe protocol [18] has become the de-facto standard for such systems because of its small overhead and support for unreliable links. Low-cost ESP32-based designs have applied the same sensing-and-actuation architecture to water and energy optimisation [19], to real-time fault monitoring of overhead power lines [20] and to the detection and reduction of standby (phantom) loads in homes [21], while lightweight protocol and encryption schemes have been proposed to secure the data exchanged by resource-constrained IoT nodes [22], [23].

Iraq and weak grids. Kazem and Chaichan [5] assessed the status and prospects of renewable energy in Iraq. Tahir et al. [6] optimised hybrid microgrids to reduce Iraq's reliance on diesel and showed that PV–battery systems are economically competitive with generators. These studies focus on sizing rather than on real-time operation. To our

knowledge, no previous study has combined an IoT implementation with an outage-schedule-aware MPC and evaluated it against common inverter rules under Iraqi supply conditions.

3. System and IoT Design

3.1. Power Architecture

Fig. 1 shows the power architecture of the studied household. An 8 kWp PV array and a 15 kWh $LiFePO_4$ battery are connected to a 6 kW hybrid inverter. The AC side of the inverter is supplied either by the national grid or by the neighbourhood generator through a changeover switch, as is common in Iraqi homes. Export to the grid is not permitted, so surplus PV is stored or curtailed. The loads are divided into base loads (air-conditioners, lighting, refrigeration and appliances) and three shiftable loads (a water pump, a washing machine and an electric water heater) that are switched by IoT relays. Table 1 lists the main parameters.

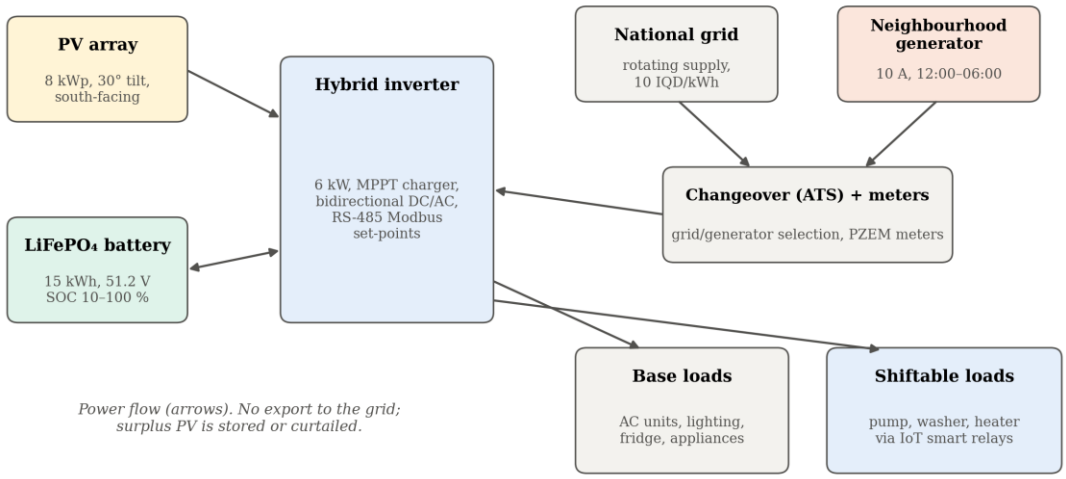


Figure 1. Power architecture of the PV–battery–grid–generator household.

Table 1. Main parameters of the studied household system (base case).

Component	Parameter	Value
PV array	Rated power; orientation	8 kWp; 30° tilt, south
PV array	Temperature coefficient; NOCT; losses	−0.35 %/°C; 45 °C; 14 %
Battery ($LiFePO_4$)	Capacity; SOC window	15 kWh; 10–100 %
Battery ($LiFePO_4$)	Power limit; charge/discharge efficiency	6 kW; 95 % / 95 %
Hybrid inverter	Rating; efficiency; export	6 kW; 96 %; not permitted
National grid	Tariff; connection limit	10 IQD/kWh; 10 kW
National grid	Supply hours (monthly mean)	10–20 h/day, rotating
Generator line	Subscription; hours; fee	10 A (2.3 kW); 12:00–06:00; 9,000 IQD/A/month
Shiftable loads	Pump; washer; water heater	1.1 kWh/day; 1.2 kWh/2 days; 3.0 kWh/day (cool days)

3.2. IoT Architecture

The IoT system follows the usual three-layer structure (Fig. 2). The perception layer consists of four ESP32 nodes. Node A measures the voltage, current, power, energy and frequency of the grid and generator feeders with two PZEM-004T energy meters. Node B communicates with the hybrid inverter over RS-485 Modbus RTU (9,600 baud, function codes 03 and 16), reads the PV, battery, grid, load and generator powers and the state of charge (SOC), and writes the time-of-use program that executes the EMS decisions (Section 5.4). The design targets the Deye hybrid inverter family, which is also sold under the Sunsynk brand and is common in Iraq; Table 4 lists the holding registers used, following the open-source register map of [24]. Node C switches the shiftable loads with solid-state relays and measures their current with split-core current transformers. Node D detects the presence of grid voltage with a ZMPT101B sensor and measures the indoor temperature.

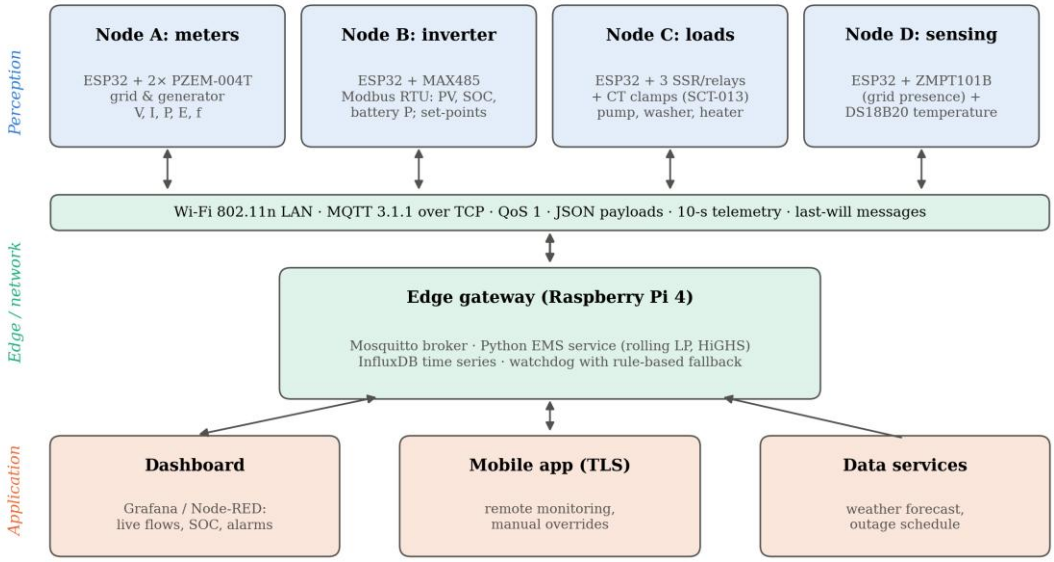


Figure 2. Three-layer IoT architecture of the energy management system.

The nodes connect over the home Wi-Fi network to an MQTT broker (Mosquitto) on a Raspberry Pi 4 edge gateway. Telemetry is published every 10 s with quality-of-service level 1, and each node registers a last-will message so that the gateway detects disconnections. The gateway stores the data in a time-series database, runs the EMS once per hour (or immediately when the grid state changes), and publishes set-points and relay commands. A watchdog switches the inverter to the rule-based outage-aware mode (strategy S2 in Section 5) if the optimiser fails or the gateway loses contact with node B. A dashboard and a mobile application provide monitoring and manual overrides; remote access is secured by TLS. Table 2 gives the bill of materials, Table 3 the MQTT topics and payloads, and Table 4 the inverter registers.

Table 2. Bill of materials of the IoT layer (indicative retail prices).

Item	Function	Qty	Cost (USD)
ESP32 DevKitC (Wi-Fi/BLE MCU)	node controller	4	24
PZEM-004T v3 (100 A CT)	grid and generator V, I, P, E, f	2	18
MAX485 RS-485 transceiver	Modbus RTU link to hybrid inverter	1	2
Solid-state relay 25 A + heat sink	switching shiftable loads	3	24
SCT-013 split-core CT	load current measurement	3	21
ZMPT101B voltage sensor	grid presence detection	1	3
DS18B20 temperature probe	indoor temperature	1	2
Raspberry Pi 4 (4 GB) + 32 GB card	MQTT broker, EMS, database	1	63
Power supplies, enclosures, wiring	installation	–	40
Total			**≈ 197**

Table 3. MQTT topics and message content (JSON payloads, QoS 1).

Topic	Publisher → subscriber	Period	Content
home/nodeA/telemetry	node A → gateway	10 s	grid and generator V, I, P, E, f, power factor
home/nodeB/telemetry	node B → gateway	10 s	PV power, battery power, SOC, inverter mode, alarms
home/nodeC/telemetry	node C → gateway	10 s	relay states, load currents
home/nodeD/telemetry	node D → gateway	10 s	grid presence flag, indoor temperature
home/nodeB/cmd	gateway → node B	1 h / event	TOU program: six slots with start time, power, SOC target, charge flags
home/nodeC/cmd	gateway → node C	1 h / event	relay on/off commands for pump, washer, heater

Topic	Publisher → subscriber	Period	Content
home/+/status	nodes → gateway	on change	online/offline (retained, last-will message)
home/ems/plan	gateway → dashboard	1 h	24-h plan: SOC trajectory, grid and generator use

Table 4. Deye/Sunsynk single-phase hybrid inverter holding registers used by node B (Modbus RTU, 9,600 baud; addresses from the open-source map [24], to be verified for the specific model and firmware).

Register	Name	R/W	Unit / encoding	Use in the EMS
184	Battery SOC	R	%	MPC initial state E_0
190	Battery power	R	W, signed	monitoring, charge/discharge check
186, 187	PV1, PV2 power	R	W	current-hour PV measurement
169	Grid power	R	W, signed	grid import
178	Load power	R	W	current-hour demand measurement
166	Gen (AUX) power	R	W	generator output
194	Grid connected	R	0/1	grid-state confirmation
219	Battery low capacity	R	%	lower bound for slot targets
248	Use Timer	W	0/1	enables the TOU program
250–255	Prog1–6 time	W	HHMM	slot start times
256–261	Prog1–6 power	W	W	slot power limit
268–273	Prog1–6 capacity	W	%	slot SOC target ($E_1/E_{\max}$ or compressed target)
274–279	Prog1–6 charge/mode	W	bit 0 grid, bit 1 gen	grid/generator charging permission

The ESP32 firmware is event-driven. Each node reads its sensors, publishes a JSON message, listens for commands on its command topic, and applies a local fail-safe. For example, node C returns to the default appliance schedule if no command is received for two hours. Reference implementations of node C (load relays) and node B (inverter interface) are given in Appendices A and B.

4. Models and Data

4.1. Weather Data

Hourly global horizontal irradiance (GHI) and 2-m air temperature for Baghdad (33.31° N, 44.37° E) for the full year 2023 were obtained from the Open-Meteo historical weather archive [25], which is based on the ERA5 reanalysis [26]. The annual GHI was 1,884 kWh/m², the maximum hourly GHI 960 W/m², and the air temperature ranged from 2.2 °C to 50.8 °C. Fig. 3 summarises the data.

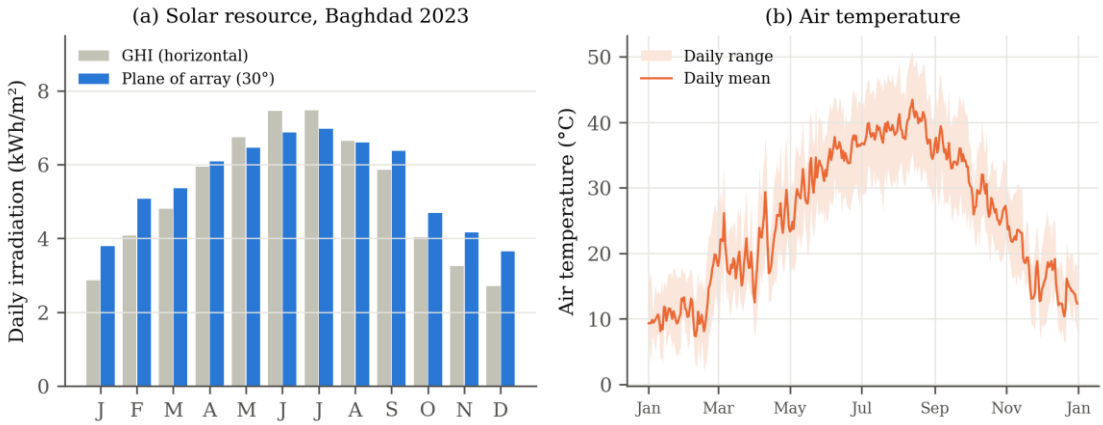


Figure 3. (a) Mean daily irradiation on the horizontal plane and on the 30° south-facing array. (b) Daily air temperature in Baghdad in 2023.

4.2. PV Model

The solar position was computed for the middle of each hour. The diffuse fraction of GHI was estimated with the Erbs correlation [27] from the clearness index k_t, and the plane-of-array irradiance G_{POA} for a 30° south-facing array was obtained with the isotropic-sky model [28]:

$$G_{\mathrm{POA}} = G_b \cos\theta + G_d \frac{1+\cos\beta}{2} + \rho\, G_h \frac{1-\cos\beta}{2} \qquad (1)$$

where G_b is the beam normal irradiance, θ the angle of incidence, G_d the diffuse horizontal irradiance, G_h the GHI, β the tilt and $\rho = 0.2$ the ground albedo. The cell temperature and AC output are

$$T_c = T_a + \frac{\mathrm{NOCT}-20}{800}\, G_{\mathrm{POA}}, \qquad P_{\mathrm{PV}} = P_{\mathrm{STC}} \frac{G_{\mathrm{POA}}}{1000} [1+\gamma(T_c-25)](1-\lambda)\,\eta_{\mathrm{inv}} \qquad (2)$$

with NOCT = 45 °C, $\gamma = -0.35\%/°\mathrm{C}$, system losses λ = 14% (including dust, which is significant in Iraq) and inverter efficiency η_{inv} = 96%. The array produced 12,036 kWh in 2023, a specific yield of 1,504 kWh/kWp. The high summer cell temperatures explain why this is lower than the irradiation alone would suggest.

4.3. Household Demand Model

Because measured appliance-level data for Baghdad households were not available, the demand was generated with a transparent bottom-up model, summarised in Table 5. The non-shiftable demand is the sum of a base load (refrigeration, network equipment and standby), lighting, cooking and appliance blocks, and temperature-driven cooling and heating:

$$P_{\mathrm{cool}}(t) = \min\{k_c\,[T_a(t)-26]^+,\ P_{c,\max}\}\, o(t), \qquad P_{\mathrm{heat}}(t) = \min\{k_h\,[15-T_a(t)]^+,\ P_{h,\max}\} \qquad (3)$$

where $o(t)$ is an occupancy factor. Correlated random variation was added through a first-order autoregressive multiplicative term with a standard deviation of 12%. Three shiftable jobs are generated each day: the water pump (1.1 kWh), the washing machine on alternate days (1.2 kWh), and the water heater on days with a mean temperature below 20 °C (3.0 kWh). Each job has a permitted window and a default start time. The resulting annual demand was 14,318 kWh, with a mean of 82 kWh/day in August and 16 kWh/day in March (Fig. 4a). These values are typical of large air-conditioned detached houses in central Iraq, although individual households vary widely.

Table 5. Bottom-up household demand model (kW unless stated; T_a in °C).

Component	Model	Notes
Base load	0.22 + 0.006 $[T_a - 25]^+$	refrigeration, router, standby
Lighting	0.25 at 18:00–23:00; 0.125 at 05:00–06:00	
Cooking and appliances	0.35 (07–08 h), 0.55 (13–14 h), 0.45 (19–21 h)	
Cooling	min{0.24 $[T_a - 26]^+$, 4.5} × occupancy	three split units
Heating	min{0.12 $[15 - T_a]^+$, 1.5}; halved at night	electric heaters
Variability	multiplicative AR(1), φ = 0.8, σ = 12 %	
Water pump (shiftable)	1.1 kWh, ≤ 0.75 kW, window 06–20 h	default start 07:00
Washing machine (shiftable)	1.2 kWh every 2nd day, ≤ 1.2 kW, 08–22 h	default start 10:00
Water heater (shiftable)	3.0 kWh if daily mean T_a < 20, ≤ 2 kW, 00–18 h	default start 05:00

4.4. Grid and Generator Model

The grid supply was modelled as a rotating schedule with monthly mean supply hours between 10 h/day in July–August and 20 h/day in March–April, consistent with the reported "two hours on, two hours off" pattern in summer [2]. The outages occur in blocks of mostly two hours, evenly spread over the day, with a starting phase that changes from day to day. The schedule is assumed to be announced one day ahead. In addition, unannounced outages of 1–4 h occur on average twice a week in summer and once a week otherwise; these are unknown to the controller. Over the year, the grid was available for 15.4 h/day on average, and 71 h of unannounced outages occurred (Fig. 4b). The neighbourhood generator line operates from 12:00 to 06:00, is used only when the grid is off, and is limited to the subscribed current (10 A, i.e. 2.3 kW at 230 V, in the base case).

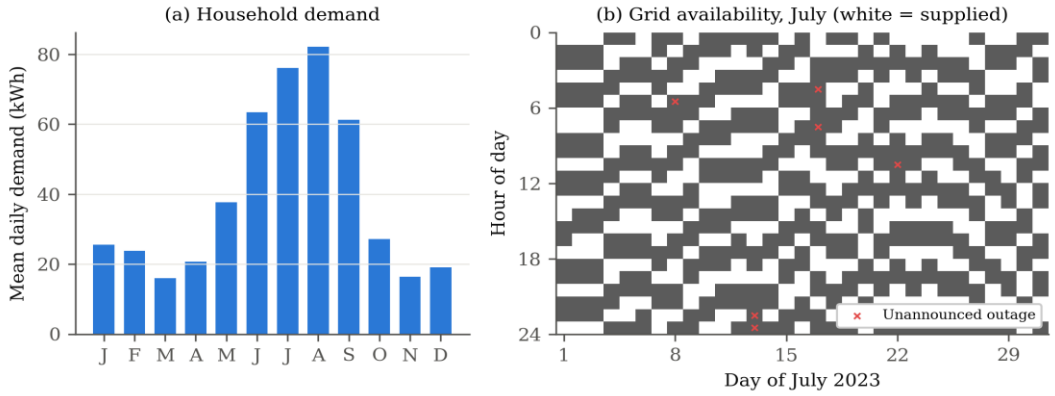


Figure 4. (a) Mean daily household demand by month. (b) Hourly grid availability in July 2023 for realisation 1 (white: grid on; grey: outage; crosses: unannounced outages).

4.5. Battery Model

The battery energy E_t evolves as

$$E_{t+1} = E_t + \eta_c P_t^c \Delta t - \frac{P_t^d}{\eta_d}\Delta t, \qquad E_{\min} \le E_t \le E_{\max} \qquad (4)$$

with charge and discharge efficiencies of 95%, power limits of 6 kW, and an SOC window of 10–100%. Battery wear is priced at 55 IQD per kWh of throughput. This value corresponds to a pack cost of 300 USD/kWh, 4,000 cycles at 90% depth of discharge and an exchange rate of 1,310 IQD/USD.

5. Energy Management Strategies

5.1. Benchmark Strategies

Six strategies were compared:

- **S0 – Grid + generator:** no PV or battery; the status quo of most households.
- **S1 – Self-use rule:** the common default of hybrid inverters. Surplus PV charges the battery, and the battery discharges whenever PV is insufficient, before the grid or generator is used. The battery is never charged from the grid.
- **S2 – Outage-aware rule:** a "backup" heuristic tailored to rotating outages. While the grid is on, the battery is kept full from PV and the grid. During an outage, the generator is used first (its fee is already paid), and the battery covers the remainder; spare generator capacity recharges the battery.
- **S3a – MPC without load shifting:** the proposed optimiser with the shiftable appliances run at their default times.
- **S3 – IoT-MPC (proposed):** the optimiser with battery dispatch and appliance scheduling through the IoT relays.
- **S4 – MPC with perfect forecasts:** S3 with perfect knowledge of PV, demand and all outages; an upper bound on what better forecasting could achieve.

5.2. Rolling-Horizon MPC Formulation

Every hour, the gateway solves a linear programme over a horizon of H = 24 h. For each step k, the decision variables are the PV used p_k^{pv}, the grid import to the loads g_k, the grid import to the battery g_k^b, the generator output q_k, the battery charge c_k and discharge d_k, the unserved energy u_k, the energy $f_{j,k}$ allocated to shiftable job j, and a reserve shortfall r_k. The objective is

$$\min \sum_{k=0}^{H-1} \left[\pi_g\left(g_k + g_k^b\right) + \pi_q q_k + \pi_w/2\left(c_k + g_k^b + d_k\right) + \pi_u u_k + \pi_r r_k\right] - \pi_E E_H \qquad (5)$$

subject to the power balance

$$p_k^{pv} + g_k + q_k + d_k + u_k = \hat{L}_k + \sum_j f_{j,k} + c_k \qquad (6)$$

the battery dynamics (4) with total charge $c_k + g_k^b$, the bounds

$$0 \le p_k^{pv} \le \hat{P}_k^{PV}, \quad 0 \le g_k, g_k^b \le \bar{G}\, a_k, \quad 0 \le q_k \le \bar{Q}\, w_k(1 - a_k), \quad c_k + g_k^b \le \bar{P}_b, \quad d_k \le \bar{P}_b \qquad (7)$$

the job constraints

$$\sum_{k \in W_j} f_{j,k} = E_j, \qquad 0 \le f_{j,k} \le \bar{F}_j \qquad (8)$$

and the soft outage reserve

$$E_{k+1} + r_k \ge E_{\min} + \frac{1}{\eta_d} \sum_{i=k+1}^{k+2} \left[1.1\,\hat{L}_i - \hat{P}_i^{PV}\right]^+, \qquad r_k \ge 0 \qquad (9)$$

Here $a_k \in \{0,1\}$ is the announced grid availability, w_k the generator operating window, $\hat{L}_k$ and $\hat{P}_k^{PV}$ the demand and PV forecasts, W_j the remaining window of job j, and E_H the terminal battery energy. The prices are π_g = 10 IQD/kWh, π_q = 1 IQD/kWh (the generator fee is fixed, so only a nominal marginal cost is used), π_w = 55 IQD/kWh, π_u = 1,000 IQD/kWh (value of lost load), π_r = 120 IQD/kWh and π_E = 15 IQD/kWh. The reserve (9) asks the controller to hold enough energy for two hours of net demand, inflated by 10%, so that an unannounced outage can be bridged; it is soft, so that it never makes the problem infeasible.

The forecasts are deliberately simple and implementable on the gateway. The PV and demand of the current hour are taken from the IoT measurements. Future hours use the value observed 24 h earlier (day-ahead persistence), and future grid availability uses the announced schedule. The problem has about 220–260 continuous variables and is solved with HiGHS [17] through SciPy [29].

5.3. Real-Time Execution

Only the decisions for the current hour are applied, and they are corrected with the measured values. PV first supplies the load, and any surplus charges the battery. When the grid is available, the battery follows the MPC set-points: the planned charge not covered by PV is drawn from the grid, and any planned discharge reduces the grid import. During an outage, the generator supplies the load up to its ampere limit, and the battery covers the remainder. Spare generator capacity may charge the battery when the plan requests it. Any demand that cannot be met is counted as unserved. The rule-based strategies use the same physical constraints, so the comparison isolates the effect of the control logic.

5.4. Execution through the Inverter's Time-of-Use Program

Commercial hybrid inverters do not usually accept direct battery power set-points from external controllers. The Deye/Sunsynk family instead offers a time-of-use (TOU) program of six slots. Each slot has a start time, a power limit, a target SOC and flags that allow charging from the grid or the generator (Table 4). The inverter firmware interprets a slot as follows: the battery supplies the load only while its SOC is above the slot target, and, if grid charging is enabled, it is charged from the grid up to the target. During a grid outage, the battery supplies the load down to its low-capacity limit regardless of the slot target.

The MPC output is mapped onto this program in two ways. In the **hourly mode (S3-TOU)**, the gateway rewrites the slot that covers the current hour every hour: the target SOC is the planned SOC at the end of the hour, $E_1/E_{\max}$, and the grid-charge flag is set if the plan contains grid charging in that hour. In the **daily mode (S3-TOU6)**, which is intended as a low-communication or fallback mode, the gateway solves the MPC once at midnight for the next 24 h and compresses the hourly SOC targets $x_1, \ldots, x_{24}$ into six slots. The slot boundaries $0 = b_0 < b_1 < \cdots < b_6 = 24$ are chosen by dynamic programming to minimise

$$J = \sum_{m=1}^{6} \sum_{h=b_{m-1}+1}^{b_m} \Big(\max_{b_{m-1} < i \le b_m} x_i - x_h ight)^2 \qquad (10)$$

and each slot receives the largest target of the hours it covers, so that the compressed program never holds less energy in reserve than the plan. A slot allows grid charging if any of its hours does. The appliance schedule of the day is sent to node C at the same time. The inverter then runs the whole day autonomously, without further commands.

5.5. Simulation Protocol and Metrics

All strategies were simulated hourly for the full year 2023, with three independent random realisations of demand variability and unannounced outages (seeds 1–3). The metrics are the unserved energy and the loss-of-power-supply probability (LPSP, unserved energy as a percentage of demand), the number of hours with unserved demand, the grid and generator energy, the PV curtailment, the battery equivalent full cycles, the PV self-consumption (share of PV production used) and self-sufficiency (share of consumption not supplied by the grid or generator), and the annual energy-service cost.

The cost is the sum of the grid bill, the generator subscription (9,000 IQD per ampere per month [3]), the battery wear and the unserved energy valued at 1,000 IQD/kWh.

6. Results

6.1. Example of Operation

Fig. 5 shows three summer days (17–19 July 2023) with the grid off for roughly half of each day. Under the self-use rule (S1), the battery is emptied every evening. Supply is then lost repeatedly during morning outages, which fall outside the generator window, and during evening outages, when demand exceeds the 2.3 kW generator limit. The outage-aware rule (S2) keeps the battery almost permanently full, which prevents unserved demand. It achieves this by recharging from the grid after every outage and by curtailing PV at midday because the battery has no room left. The proposed IoT-MPC (S3) keeps the SOC between about 50% and 95%. It discharges to cover outages, uses the generator within its window, and leaves room to absorb midday PV, recharging from the grid only as much as the next announced outages and the reserve require.

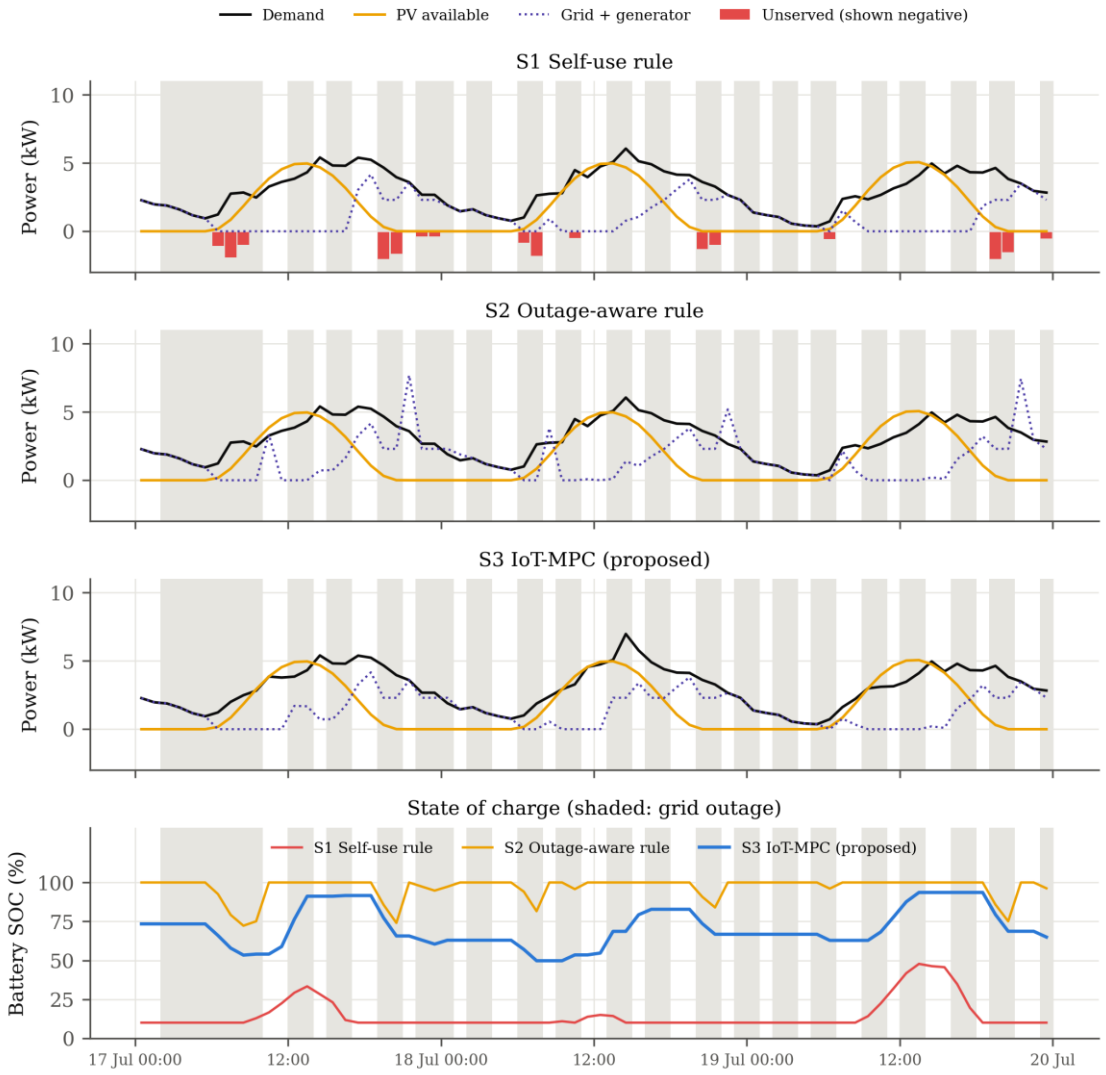


Figure 5. Operation on 17–19 July 2023 (realisation 1) under S1, S2 and S3. Shaded bands mark grid outages; unserved demand is shown as negative bars.

6.2. Annual Performance

Table 6 summarises the annual results (mean over three realisations), and Fig. 6 shows the annual supply mix.

Table 6. Annual performance of the control strategies (mean over three realisations; demand 14,318 kWh/year). The standard deviation across realisations was below 3.5% of the mean for all quantities except the unserved energy, which is given as mean ± standard deviation.

Strategy	Unserved (kWh)	LPSP (%)	Hours unserved	Grid (kWh)	Gen. (kWh)	Curtailed (kWh)	Cycles	Self-cons. (%)	Self-suff. (%)	Cost (M IQD)
S0 Grid + generator	2,940.3 ± 50.2	20.42	1,664	8,091	3,369	0	0.0	0.0	0.0	4.101
S1 Self-use rule	918.4 ± 21.2	6.38	705	2,406	1,602	2,233	224.3	81.4	71.0	2.198
S2 Outage-aware rule	0.0 ± 0.0	0.00	0	5,545	2,420	5,479	77.7	54.5	45.2	1.196
S3a MPC, no load shifting	1.1 ± 1.4	0.01	2	4,753	2,625	4,892	77.6	59.4	49.2	1.190
S3 IoT-MPC (proposed)	0.2 ± 0.3	0.00	0	4,235	2,629	4,399	63.8	63.5	52.7	1.173
S4 MPC, perfect forecast	0.0 ± 0.0	0.00	0	4,176	2,645	4,356	63.7	63.8	53.0	1.172

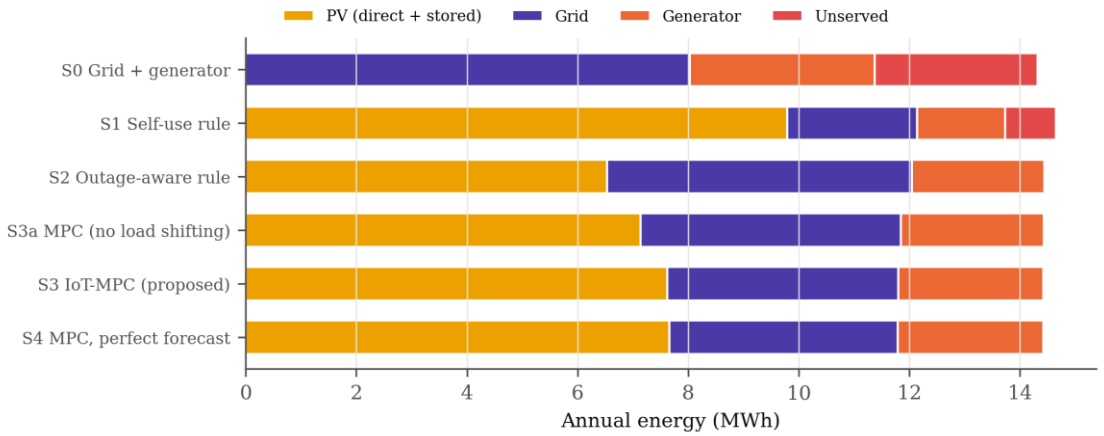


Figure 6. Annual supply mix by strategy (realisation 1).

Without PV and storage (S0), 2,940 kWh, or 20.4% of the demand, could not be served, spread over about 1,660 hours per year. This reflects outages outside the generator window and demand above the 10 A limit. Adding PV and a battery under the self-use rule (S1) cut the unserved energy to 918 kWh (6.4%) and achieved the highest self-sufficiency (71%), but it still left about 700 hours of interrupted supply. Self-use is therefore unsuitable for Iraqi conditions, even though it is the default mode of many inverters.

Both the outage-aware rule (S2) and the proposed IoT-MPC (S3) served practically the entire demand: less than 1 kWh of unserved energy per year in all realisations. They differ markedly in how they achieve this. Relative to S2, the IoT-MPC reduced grid imports by 23.6% (from 5,545 to 4,235 kWh), PV curtailment by 19.7% (from 5,479 to 4,399 kWh) and battery cycling by 17.9% (from 77.7 to 63.8 equivalent full cycles). It raised PV self-consumption from 54.5% to 63.5% and self-sufficiency from 45.2% to 52.7%. Generator energy rose by 8.6%, because the optimiser uses the prepaid generator during its window to preserve battery energy for outages outside it. The annual cost fell by 2.0%, from 1.196 to 1.173 million IQD.

The ablation S3a shows the contribution of IoT load shifting. Without it, the MPC still reduced grid imports by 14.3% relative to S2. Scheduling the pump, washer and water heater into PV-rich or grid-available hours reduced grid imports by a further 10.9%, curtailment by 10.1% and battery cycling by 17.8%. Finally, the proposed controller came within 1.4% of the grid import and 0.1% of the cost of the MPC with perfect forecasts (S4). Simple persistence forecasts are therefore sufficient in Baghdad's stable climate, as long as the soft reserve protects against unannounced outages.

6.3. Seasonal Behaviour

Fig. 7 shows the monthly unserved energy and self-sufficiency. Losses of supply under S0 and S1 peak in July–August, when the grid supplies only about 10 h/day and air-conditioning demand is highest. The outage-aware rule and the IoT-MPC served all demand in every month. Their self-sufficiency differs most in winter, when S2 keeps the battery full from the grid, whereas S3 leaves room for the next day's PV. In December, S3 reached 50% self-sufficiency against 25% for S2.

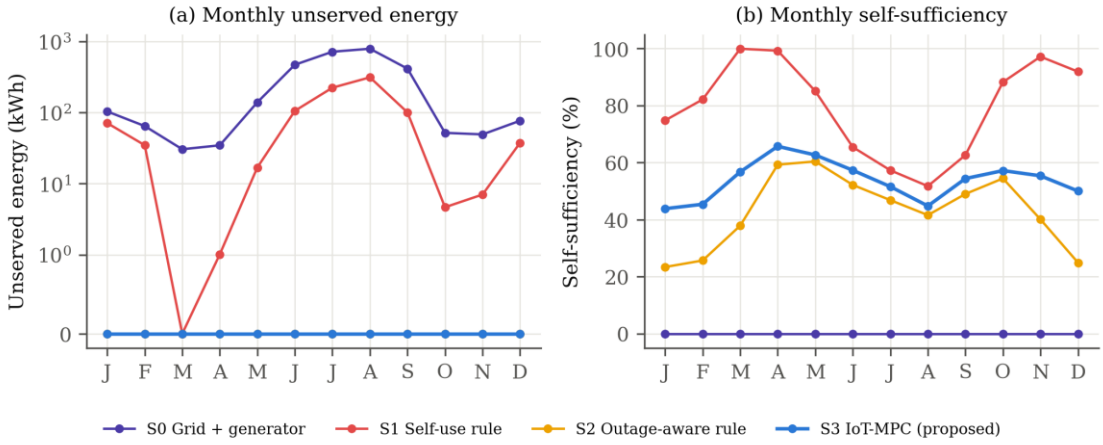


Figure 7. (a) Monthly unserved energy (symmetric logarithmic scale; S2 and S3 coincide at zero). (b) Monthly self-sufficiency (realisation 1).

6.4. Battery Utilisation

Fig. 8 compares the SOC distributions. Under S1, the battery spends most of the time at its lower limit, so it is empty when it is needed. Under S2, it spends most of the time near 100%, which accelerates calendar ageing of lithium-ion cells and wastes PV. Under S3, the SOC is spread over the mid-range, which is both healthier for the battery and better aligned with the purpose of storage: to move PV energy and grid energy into outage periods.

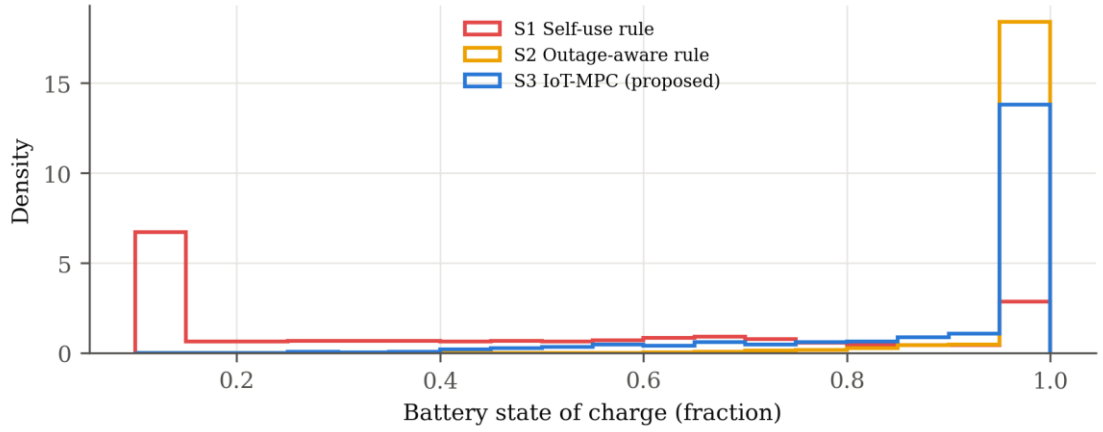


Figure 8. Distribution of the battery state of charge over the year (realisation 1).

6.5. Sizing of Battery and Generator Subscription

Fig. 9 and Table 7 show the LPSP and annual cost for battery capacities of 5–20 kWh and generator subscriptions of 5–15 A (realisation 1). The generator subscription dominates the annual cost: each ampere costs 108,000 IQD per year, whereas the grid bill is only about 40,000–65,000 IQD per year. Halving the subscription from 10 A to 5 A therefore lowers the cost by about 40%, provided the battery can bridge the larger deficit. With a 10 kWh battery and a 5 A line, the IoT-MPC served 99.77% of the demand at an annual cost of 0.715 million IQD, compared with 1.177 million IQD at 10 A. With 20 kWh, it served 99.93% at 0.692 million IQD.

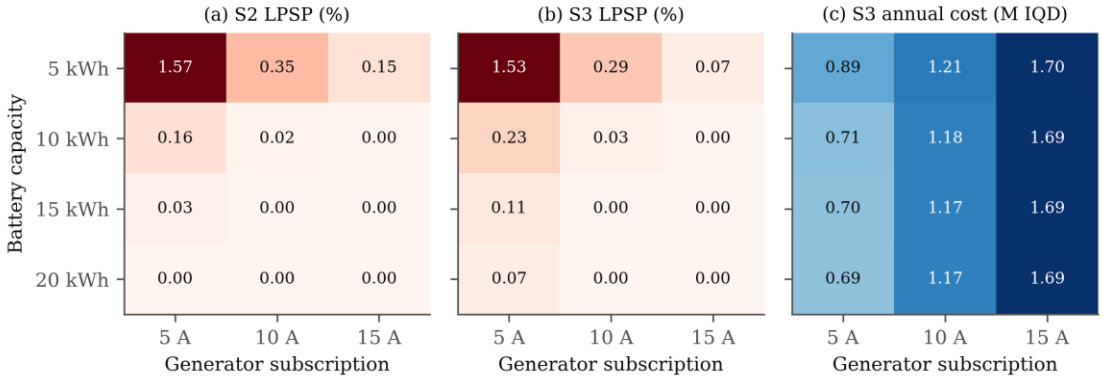


Figure 9. Sensitivity of (a) the LPSP of S2, (b) the LPSP of S3 and (c) the annual cost of S3 to battery capacity and generator subscription (realisation 1).

Table 7. LPSP (%) and annual cost (million IQD) of S2 and S3 for different battery capacities and generator subscriptions (realisation 1).

Battery	Subscription	S2 LPSP	S3 LPSP	S2 cost	S3 cost	S3 grid (kWh)	S3 cycles
5 kWh	5 A	1.57	1.53	0.919	0.890	5,047	309
5 kWh	10 A	0.35	0.29	1.243	1.213	4,453	182
5 kWh	15 A	0.15	0.07	1.731	1.699	4,114	108
10 kWh	5 A	0.16	0.23	0.732	0.715	4,984	175
10 kWh	10 A	0.02	0.03	1.199	1.177	4,281	95
10 kWh	15 A	0.00	0.00	1.711	1.689	4,032	55
15 kWh	5 A	0.03	0.11	0.714	0.697	4,911	118
15 kWh	10 A	0.00	0.00	1.197	1.172	4,180	64
15 kWh	15 A	0.00	0.00	1.711	1.689	3,983	37
20 kWh	5 A	0.00	0.07	0.711	0.692	4,892	89
20 kWh	10 A	0.00	0.00	1.197	1.172	4,178	48
20 kWh	15 A	0.00	0.00	1.711	1.689	3,976	28

The sensitivity analysis also shows the limits of the proposed controller. With a very small battery (5 kWh), the MPC was more reliable than the rule at every subscription level, because it plans the scarce stored energy across successive outages. With a 5 A line and a battery of 10 kWh or more, however, the “always full” rule was slightly more reliable (for example, LPSP 0.03% versus 0.11% at 15 kWh). In this tightly constrained case, the MPC’s economy (less grid charging, more room for PV) occasionally leaves too little energy for an unannounced outage. A larger reserve weight or a longer reserve period would close this gap at the cost of some of the grid savings. This trade-off should be exposed to the user as a configurable setting.

6.6. Effect of Tariff Reform

Iraq’s residential tariffs are far below cost-recovery levels, and reforms have been discussed repeatedly [4]. Fig. 10 shows the annual cost of S2 and S3 for grid prices of 10, 35 and 80 IQD/kWh. Because the MPC reacts to prices, its advantage grows with the tariff: from 2.0% at 10 IQD/kWh to 4.3% at 35 IQD/kWh and 10.2% at 80 IQD/kWh. At the highest price, the optimiser cut grid imports by 66% relative to S2, shifting supply towards PV, the prepaid generator and the battery. This increased battery cycling about threefold, to 236 cycles per year, and generator energy by 33%. These side effects, discussed in Section 7, show that the objective weights should reflect environmental as well as financial costs.

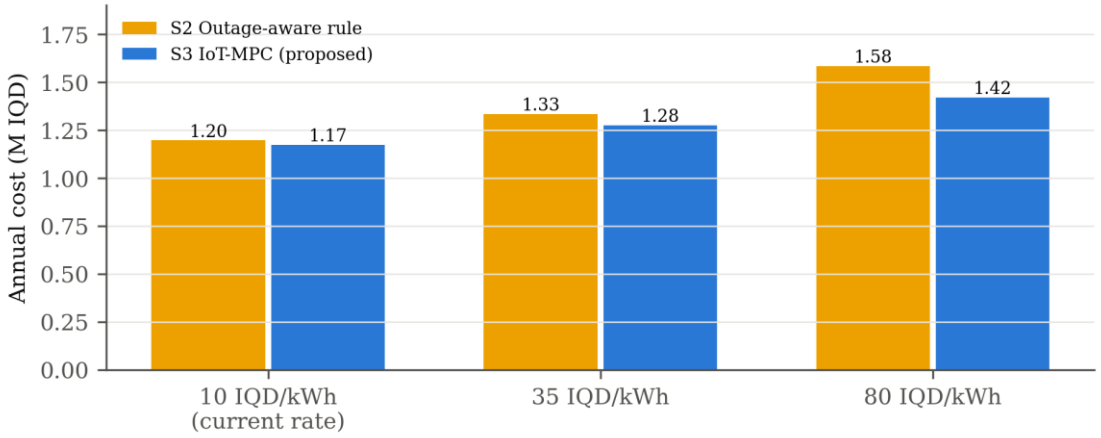


Figure 10. Annual energy-service cost of the outage-aware rule (S2) and the IoT-MPC (S3) under three grid tariffs (realisation 1, 15 kWh battery, 10 A subscription).

6.7. Execution on the Inverter Timer

Table 8 compares the ideal set-point execution of the MPC with the two TOU execution modes. The hourly TOU mode reproduced the set-point results to within 0.1 kWh per year in every quantity. Hence the inverter's own control logic, driven by an hourly SOC target and a grid-charge flag, is sufficient to realise the optimised schedule, and no modification of the inverter firmware is needed. The daily six-slot mode, which needs only one write sequence per day, still served 99.98% of the demand (3.5 kWh unserved per year over about four hours). It drew 21% less energy from the grid and achieved a higher self-sufficiency of 59.5%. This came at the price of more than twice the battery cycling (144 equivalent full cycles per year) and a 4.9% higher annual cost. The reason is the inverter's TOU logic: a slot target that is held constant for several hours lets the battery discharge whenever its SOC exceeds that target, even while the grid is available. The daily mode is therefore a sound fallback when the gateway or the network is unavailable, whereas the hourly mode should be used in normal operation.

Table 8. Ideal set-point execution of the MPC versus execution through the inverter TOU program (mean over three realisations).

Execution mode	Unserved (kWh)	Hours unserved	Grid (kWh)	Gen. (kWh)	Curtailed (kWh)	Cycles	Self-suff. (%)	Cost (M IQD)	Commands per day
Ideal set-points (S3)	0.2	0.3	4,235	2,629	4,399	63.8	52.7	1.173	24
TOU, hourly rewrite (S3-TOU)	0.2	0.3	4,235	2,629	4,399	63.8	52.7	1.173	24
TOU, daily 6 slots (S3-TOU6)	3.5	3.7	3,351	2,569	3,345	143.8	59.5	1.230	1

6.8. Computational and Communication Load

Table 9 summarises the computing and network requirements. Each hourly optimisation was solved in 4.8 ms on average and 35 ms in the worst case on a two-core virtual CPU, so even a Raspberry Pi, which is several times slower, would complete it in well under a second. The telemetry of the four nodes amounts to about 8.9 MB per day, or 0.82 kbit/s on average, which is negligible for a home Wi-Fi network and allows operation over a mobile data connection if required.

Table 9. Computational and communication requirements of the IoT-MPC.

Quantity	Value
LP size per solve	≈ 220–260 variables, ≈ 100–130 constraints
Solve time, mean / maximum (2-core virtual CPU)	4.8 ms / 35 ms
Optimisations per year	8,760 (hourly)
Telemetry messages per day	4 nodes × 8,640 = 34,560

Quantity	Value
Telemetry volume	≈ 8.9 MB/day (0.82 kbit/s average)
Command messages per day	≈ 48 (set-points and relay commands)
Fail-safe	rule S2 on gateway fault; default appliance times on node timeout (2 h)

7. Discussion

Why does optimisation help? In a reliable grid, the value of a residential battery comes mainly from price arbitrage and self-consumption. Under rotating outages, its main value is reliability, and the simplest way to obtain reliability is to keep the battery full. The results confirm that this rule (S2) is effective: it eliminated unserved energy in the base case. Its cost is hidden in other quantities, namely a quarter more grid import, a fifth more PV curtailment, more battery cycling and permanently high SOC. The MPC achieves the same reliability with less of each because it knows the announced schedule and therefore how much energy the next outages will require. The IoT layer is essential to this result: it provides the grid-state signal, the current measurements that correct the forecasts, and the relays that move shiftable loads into favourable hours.

Implications for households and the grid. For an individual household under today's subsidised tariff, the financial gain of MPC over a well-designed rule is modest (about 24,000 IQD per year). The larger economic lever is sizing: a PV–battery system controlled by either strategy allows the generator subscription to be halved, saving roughly 0.5 million IQD per year. The system-level benefit of MPC is more significant. A 24% reduction in grid imports by households with batteries, multiplied over many homes, would reduce the peak load on an overstretched grid. Most of the avoided grid energy is battery charging immediately after outages, which coincides with the moments when distribution feeders are most heavily loaded. If tariffs are reformed, the household's financial incentive to adopt MPC also rises.

Environmental trade-off. Because the generator fee is fixed, a cost-minimising controller treats generator energy as almost free. This increased generator use by 9% in the base case and by 33% in the high-tariff scenario. Assigning a marginal cost to generator energy, representing fuel, noise and emissions, would reduce this effect at little cost to reliability. Generator operators that bill by energy rather than by ampere would create the same incentive.

Limitations. (i) The demand, outage and generator profiles are modelled rather than measured; they are calibrated to reported conditions but do not represent any specific household. (ii) The hardware design and firmware were not deployed in a field prototype; the evaluation is a simulation driven by real weather data, and practical issues such as Wi-Fi reliability, inverter communication protocols and sensor accuracy remain to be validated experimentally. (iii) Hourly resolution cannot capture inverter power limits during short demand peaks or the start-up currents of air-conditioners. (iv) Only one PV size and one climate were studied, and the forecasts did not use weather predictions, which AI-based PV forecasting methods could supply [14]. (v) The changeover between grid and generator was assumed instantaneous. (vi) The inverter's TOU behaviour was modelled from its documented semantics; register addresses and slot semantics can differ between Deye/Sunsynk models and firmware versions and must be verified on the target unit before the controller is used.

8. Conclusion

This paper presented an IoT-based energy management system for hybrid PV–battery–grid residential systems under intermittent grid supply, with a complete hardware, network and software design and an outage-aware model-predictive controller. A full-year simulation for a Baghdad household with real 2023 weather data showed that the default self-use inverter mode leaves 6.4% of the demand unserved. Both an outage-aware rule and the proposed IoT-MPC serve practically all demand. Compared with the rule, the IoT-MPC reduced grid imports by 24%, PV curtailment by 20% and battery cycling by 18%, and it raised self-sufficiency by 7.5 percentage points. Load shifting through IoT relays contributed about half of the grid saving. Executed through the six-slot time-of-use program of a Deye/Sunsynk inverter, rewritten hourly, the controller reproduced these results exactly without any change to the inverter firmware. The controller's performance was within about 1% of an MPC with perfect forecasts, and its computational and communication requirements are small enough for low-cost edge hardware. A sizing analysis showed that a PV–battery system allows the generator subscription to be halved, reducing the annual energy-service cost by about 40%, and the cost advantage of MPC grows to 10% under a reformed tariff.

Future work will field-test the prototype on a Deye-based laboratory installation and in a Baghdad home, replace persistence forecasts with weather-based forecasts, extend the controller to minute-level control of air-conditioning loads, and study the aggregated effect of many such systems on distribution feeders.

Funding or Acknowledgment

The author received no external funding for this study.

Conflicts of Interest

The author declares no conflicts of interest.

Data Availability

The weather data were obtained from the publicly accessible Open-Meteo historical weather archive [25]. The simulation code, models and firmware can be provided by the corresponding author on reasonable request.

References

[1] International Energy Agency, *Iraq's Energy Sector: A Roadmap to a Brighter Future*, Paris: IEA, 2019.

[2] 964media, "Electricity cuts worsen across Iraq as summer heat arrives," 2025. [Online]. Available: https://en.964media.com/47717/

[3] Shafaq News, "Fuel allocation and rising ampere prices: Iraq grapples with chronic summer power shortages," June 2023. [Online]. Available: https://shafaq.com/en/Report/Fuel-allocation-and-rising-ampere-prices-Iraq-grapples-with-chronic-summer-power-shortages

[4] Iraq Business News, "No change to Iraq's subsidized electricity prices," 10 December 2025. [Online]. Available: https://www.iraq-businessnews.com/2025/12/10/no-change-to-iraqs-subsidized-electricity-prices/

[5] H. A. Kazem and M. T. Chaichan, "Status and future prospects of renewable energy in Iraq," *Renewable and Sustainable Energy Reviews*, vol. 16, no. 8, pp. 6007–6012, 2012.

[6] K. A. Tahir, J. Nieto, C. Díaz-López, and J. Ordóñez, "From diesel reliance to sustainable power in Iraq: Optimized hybrid microgrid solutions," *Renewable Energy*, vol. 238, 121905, 2025, doi: 10.1016/j.renene.2024.121905.

[7] B. Zhou, W. Li, K. W. Chan, Y. Cao, Y. Kuang, X. Liu, and X. Wang, "Smart home energy management systems: Concept, configurations, and scheduling strategies," *Renewable and Sustainable Energy Reviews*, vol. 61, pp. 30–40, 2016.

[8] H. Shareef, M. S. Ahmed, A. Mohamed, and E. Al Hassan, "Review on home energy management system considering demand responses, smart technologies, and intelligent controllers," *IEEE Access*, vol. 6, pp. 24498–24509, 2018.

[9] M. Pipattanasomporn, M. Kuzlu, and S. Rahman, "An algorithm for intelligent home energy management and demand response analysis," *IEEE Transactions on Smart Grid*, vol. 3, no. 4, pp. 2166–2173, 2012.

[10] A. Parisio, E. Rikos, and L. Glielmo, "A model predictive control approach to microgrid operation optimization," *IEEE Transactions on Control Systems Technology*, vol. 22, no. 5, pp. 1813–1827, 2014.

[11] D. Mariano-Hernández, L. Hernández-Callejo, A. Zorita-Lamadrid, O. Duque-Pérez, and F. Santos García, "A review of strategies for building energy management system: Model predictive control, demand side management, optimization, and fault detect & diagnosis," *Journal of Building Engineering*, vol. 33, 101692, 2021.

[12] A. R. Al-Ali, I. A. Zualkernan, M. Rashid, R. Gupta, and M. Alikarar, "A smart home energy management system using IoT and big data analytics approach," *IEEE Transactions on Consumer Electronics*, vol. 63, no. 4, pp. 426–434, 2017.

[13] R. Luthander, J. Widén, D. Nilsson, and J. Palm, "Photovoltaic self-consumption in buildings: A review," *Applied Energy*, vol. 142, pp. 80–94, 2015.

[14] H. A. Mutar, I. J. Mohammed, and I. R. N. ALRubeei, "AI for solar PV forecasting, MPPT, and energy management: A comprehensive review," *International Journal of Computational and Electronic Aspects in Engineering*, vol. 7, no. 1, pp. 100–114, 2026, doi: 10.26706/ijceae.7.1.20260111.

[15] A. A. Hadi, "The impact of artificial neural network (ANN) on the solar energy cells: A review," *International Journal of Computational and Electronic Aspects in Engineering*, vol. 5, no. 1, pp. 30–41, 2024, doi: 10.26706/ijceae.5.1.20240505.

[16] M. Kadhim, "Improving power quality with active filtering and energy storage technologies in grid-connected hybrid solar-wind renewable energy systems," *International Journal of Computational and Electronic Aspects in Engineering*, vol. 7, no. 2, pp. 291–304, 2026, doi: 10.26706/ijceae.7.2.20260317.

[17] Q. Huangfu and J. A. J. Hall, "Parallelizing the dual revised simplex method," *Mathematical Programming Computation*, vol. 10, no. 1, pp. 119–142, 2018.

[18] OASIS, *MQTT Version 3.1.1*, OASIS Standard, 2014.

[19] I. A. Ameen and M. A. Al-Sheikh, "Wireless sensor networks for smart gardening: ESP-NOW and Blynk IoT integration for water and energy optimization," *International Journal of Computational and Electronic Aspects in Engineering*, vol. 5, no. 3, pp. 101–115, 2024, doi: 10.26706/ijceae.5.3.20240804.

[20] O. A. Abdaumran, "IoT-enabled real-time fault monitoring in overhead power lines using ESP32 and Arduino integrated development," *International Journal of Computational and Electronic Aspects in Engineering*, vol. 6, no. 3, pp. 190–201, 2025, doi: 10.26706/ijceae.6.3.20250610.

[21] S. Waghe, U. Kuradkar, S. Prajapati, and R. Mohane, "Detecting and reducing phantom power: A human-centric IoT approach," *International Journal of Computational and Electronic Aspects in Engineering*, vol. 7, no. 3, pp. 76–83, 2026, doi: 10.26706/ijceae.7.3.20260711.

[22] A. W. Talab, "Improving communication protocols based on crucial data transmission security for IoT techniques," *International Journal of Computational and Electronic Aspects in Engineering*, vol. 6, no. 1, pp. 1–11, 2025, doi: 10.26706/ijceae.6.1.20250203.

[23] S. Q. Ameen, R. G. S. Alsulta, Z. S. Hussain, and Z. T. Abdul-Rahmman, "A hybrid RSA–ElGamal framework for secure end-to-end communications in resource-constrained IoT networks," *International Journal of Computational and Electronic Aspects in Engineering*, vol. 7, no. 2, pp. 140–153, 2026, doi: 10.26706/ijceae.7.2.20260303.

[24] J. Kellerman, "sunsynk: Deye/Sunsynk hybrid inverter Modbus library and register definitions," open-source software (Apache-2.0), GitHub, 2026. [Online]. Available: https://github.com/kellerza/sunsynk

[25] P. Zippenfenig, "Open-Meteo.com Weather API," Zenodo, 2023, doi: 10.5281/zenodo.7970649.

[26] H. Hersbach *et al.*, "The ERA5 global reanalysis," *Quarterly Journal of the Royal Meteorological Society*, vol. 146, no. 730, pp. 1999–2049, 2020.

[27] D. G. Erbs, S. A. Klein, and J. A. Duffie, "Estimation of the diffuse radiation fraction for hourly, daily and monthly-average global radiation," *Solar Energy*, vol. 28, no. 4, pp. 293–302, 1982.

[28] J. A. Duffie and W. A. Beckman, *Solar Engineering of Thermal Processes*, 4th ed. Hoboken, NJ: Wiley, 2013.

[29] P. Virtanen *et al.*, "SciPy 1.0: Fundamental algorithms for scientific computing in Python," *Nature Methods*, vol. 17, pp. 261–272, 2020.